Article:
Irisawa, K., Garcia-Lodeiro, I. and Kinoshita, H. orcid.org/0000-0001-8805-1774 (2020) Influence of mixing solution on characteristics of calcium aluminate cement modified with sodium polyphosphate. Cement and Concrete Research, 128. 105951. ISSN 0008-8846

https://doi.org/10.1016/j.cemconres.2019.105951

Influence of Mixing Solution on Characteristics of Calcium Aluminate Cement Modified with Sodium Polyphosphate

Keita Irisawa[a,*], Inés Garcia-Lodeiro[b,c], Hajime Kinoshita[b]

[a] *Sector of Decommissioning and Radioactive Waste Management, Japan Atomic Energy Agency, Tokai, Japan*

[b] *Department of Materials Science and Engineering, University of Sheffield, Sheffield, UK*

[c] *Department of Materials, Eduardo Torroja Institute (IETcc-CSIC), Madrid, Spain*

Abstract

This study investigated characteristics of a calcium aluminate cement modified with a phosphate (CAP) by changing an amount and concentration of mixing solution with sodium polyphosphate. When the amount of mixing solution was increased with a constant amount of sodium polyphosphate, an enhanced consumption of monocalcium aluminate was observed compared with gehlenite in calcium aluminate cement. Formation of gibbsite, $Al(OH)_3$, was also increased as a hydration product in the CAP and a reduction of water in the amorphous gel phase. When the amount of mixing solution was increased with a constant concentration of sodium polyphosphate, the enhanced consumption of monocalcium aluminate was not observed. Neither gibbsite nor any other crystalline hydration products were identified in this series. In addition, unreacted sodium polyphosphate remained in the system. The increased formation of gibbsite and the possible reduction of water from the amorphous gel phase appears to contribute to the improvement of the microstructure in the products.

Keywords: Calcium Aluminate Cement (CAC), Sodium Polyphosphate, Phosphate Cement, Mixing solution

[*]Corresponding author
E-mail address: irisawa.keita@jaea.go.jp (K. Irisawa)

1. Introduction

Chemically-bonded phosphate cements and ceramics can have a wide range application, from the technical cements such as dental cements [1] and shielding material for neutrons or immobilizing matrix for highly radioactive fission products [2], to the products as common as the construction cements and the corrosion and fire protection coatings [3].

Calcium aluminate cement (CAC) modified with phosphates are a type of chemically-bonded phosphate cements, and can be found in various studies. CAC modified with ammonium polyphosphate was investigated by Sugama and Callciero as an alternative for the magnesium phosphate cement system that experiences a hydrolytic deterioration [4]. They later improved their system by replacing the ammonium phosphates to sodium phosphates as the environmentally safe reactant [5] to avoid the potential emission of NH_3 gas. Ma and Brown used sodium phosphates to modify CAC hydration, as a means to suppress the formation of metastable CAH_{10} and C_2AH_8 and avoid the consequent conversion reaction into stable C_3AH_6 [6,7].

The well-known characteristics of the CAC modified with phosphates (CAP) are; rapid setting [8], high mechanical strength [9] and relatively low internal pH [10]. Taking these characteristics into account, the CAP was investigated for solidification/stabilization of toxic metal solutions as an alternative of ordinary Portland cement [11]. CAP systems have also been investigated for cementation of radioactive wastes [12] including the aqueous secondary wastes arising from the water treatment of Fukushima Daiichi Nuclear Power Stations [13].

The CAP usually consists of anhydrous CAC powder, phosphate powder(s) and mixing water. It is considered that the CAC hardens together with phosphate component

through the acid-base reaction [9]. Compositional effects on the characteristics of the CAP systems have been investigated, but the focus of the investigations have been on the phosphate components, either the types of phosphates [12] or the amount of the added phosphates against a fixed composition of CAC system [8]. The effects of the mixing solution with varied phosphate and water amounts on the characteristics of the CAP have not been openly reported, despite the significance of water contents in the properties of cementitious systems. Numbers of studies on the water contents can be found for the other cement systems [14-17].

The present study focused on the amount of mixing solution in the CAP system. Based on the formulation in the literature [9], CAC was modified with a sodium polyphosphate, but the amount of mixing solution was altered with a constant amount of sodium polyphosphate (a constant phosphate to CAC ratio) or a constant concentration of sodium polyphosphate (a constant phosphate to water ratio), and their effects on the reaction of CAC clinker phases, resulting product phases and basic microstructure of the hardened products were examined.

2. Experimental

2.1. Materials

Secar® 51 supplied by Kerneos Ltd. was used as the basis of the binders studied in the present study, combined with reagent grade of sodium polyphosphate, $(NaPO_3)_n$ (65-70%, Acros Organics Ltd.). The oxide composition of Secar® 51 is shown in **Table 1** [13]. Distilled water was used for dissolution of sodium polyphosphate and then mixed with CAC.

2.2. Sample synthesis and testing procedures

Sodium polyphosphate powders were premixed with distilled water on a roller mixer for 24 h at room temperature. The mixed solution was then added to the Secar® 51 powder during the initial hand mixing of 30 s, followed by the shear mixing using a Silverson L4RT high shear mixer for 120 s at 2,500 rpm to form a homogenous paste. After mixing, the paste was cured in a sealed plastic centrifuge tube at 20°C for 28 days. **Table 2** shows the compositions of the CAP samples studied in the present study. In the Table 2, cement, sodium polyphosphate and distilled water were abbreviated as "c", "p" and "w", respectively. The "p/c", "p/w" and "w/c" were shown as their weight ratios.

The composition of the reference sample (CAP_{ref}) is the same as that reported by Chavda *et al.* [9], and composed of 100 g of the Secar® 51 (hereinafter, referred to as "c"), 40 g of sodium polyphosphate (hereinafter, referred to as "p") and 35 g of distilled water (hereinafter, referred to as "w"). Based on the reference composition, the amount of mixing solution was altered in two different ways; with a constant amount of sodium polyphosphate (at a constant p/c ratio of 0.40 g/g) or a constant concentration of sodium polyphosphate (at a constant p/w ratio of 1.14 g/g). For the p/c = 0.40 series (0.40p/c series), the CAP samples were called CAP_{50w}, CAP_{75w}, and CAP_{100w} when the mixing water increased to 50, 75, and 100 g, respectively. For the p/w = 1.14 series (1.14p series), the CAP samples were called CAP_{57p}, CAP_{86p}, and CAP_{114p} based on the increased amount of phosphate to maintain the concentration of phosphate constant when the mixing water increased to 50, 75, and 100 g, respectively.

After 28 days of curing, the samples were crushed into roughly <1 cm^3 pieces and immersed in acetone for a few days. Samples were then air dried at room temperature for 24 h, followed by a vacuum desiccation at ca. 50 torr to prevent potential carbonation.

Some of the pieces were mounted in an epoxy resin and surface polished to analyse the microstructure of the resulting cement pastes by scanning electron microscopy with energy-dispersive X-ray (SEM/EDX) using a HITACHI TM3030. Remaining samples were further ground and sieved to <63 μm for X-ray diffraction (XRD) analysis with a Siemens D500 diffractometer (Cu K_α radiation). Thermogravimetric analysis (TGA) was also carried out, with powdered samples heated from room temperature up to 1,000°C at 10°C min^{-1} in a N_2 flow (200 cm^3/min.), using a Perkin-Elmer TG analyser. The attenuated total reflection / Fourier transform infrared spectroscopy (ATR/FT-IR) was also carried out, with <63 μm of powdered samples as mentioned above using a Perkin-Elmer Frontier Optica.

3. Results and discussion

3.1. Effect of water on reaction of CAC clinkers

Figure 1 shows the X-ray diffractograms for the samples. Well defined and intense reflections of the crystalline calcium aluminate clinker phases were observed in the diffractogram of the CAP_{ref}, indicating monocalcium aluminate, CA ($CaAl_2O_4$, pattern diffraction file PDF #01-070-0134), gehlenite, C_2AS ($Ca_2Al_2SiO_7$, PDF #00-035-0755), and calcium titanate, CT ($CaTiO_3$, PDF #01-075-2100). In good agreement with the other reports [8,9,12,13], the CAP_{ref} shows no obvious reflection for either the conventional hydration products observed in hydrated CAC or any crystalline phases other than the anhydrous clinker phases [8,9,12]. The phosphate modification is altering the reaction pathway, avoiding the conventional CAC hydration and mitigating potential issues surrounding the conversion reaction throughout the 28 days of curing period.

However, in the 0.40p/c series, a presence of gibbsite, AH_3 ($Al(OH)_3$, PDF#00-012-0401), a stable hydration product in the conventional CAC was observed in the formulations with 0.75 and 1.00 of w/c ratio (CAP_{75w} and CAP_{100w}), but hydrogarnet, C_3AH_6 ($Ca_3Al_2O_6{\cdot}6H_2O$, PDF#00-024-0217), the other stable hydration product in the conventional CAC was not formed in CAP_{50w}, CAP_{75w} and CAP_{100w}. The peaks of AH_3 (18.2 and 20.2°) clearly intensified when the w/c ratio increased in the 0.40p/c series. On the other hand, the intensity of the main peak assigned to CA (29.9°) decreased with increasing w/c ratio, and those assigned to C_2AS (31.2°) indicated little change, suggesting the enhanced reaction of CA and limited reaction of C_2AS under this condition. The 1.14p/w series indicated a very similar behaviour to the reference system. The peak corresponding to Aluminium phosphate, $AlPO_4$ (27.65°) [18] was not detected. Neither the formation of stable CAC hydration products (AH_3 or C_3AH_6) nor enhanced reaction of CA was observed in their XRD data.

Figure 2 shows the peak intensity ratio of the main peaks for CA (29.9°) and C_2AS (31.2°) as a function of w/c ratio of the system. The circle and square data points show the 0.40p/c series and the 1.14p/w series, respectively. The correlation coefficients (R^2) of the 0.40p/c and the 1.14p/w series were 0.96 and 0.01 by a least-square method, respectively. The small R^2 value for the 1.14p/w series is due to the constant value of the data points, indicating the limited relevance of the linear fitting. Although the simple comparison of XRD peaks would not allow to conduct a precise quantitative analysis, the data presented here can show general trends. For the 0.40p/c series, the peak intensity ratio of CA/C_2AS appears to be linearly correlated with an increase of the w/c ratio. On the other hand, for the 1.14p/w series, the peak intensity ratio of CA/C_2AS did not change. These results suggest that the consumption of CA increases with the increase in the w/c

ratio, but it does not change when the concentration of sodium polyphosphate in the solution is constant.

It should be noted that the enhanced dissolution of CA and formation of AH_3 could be related, but not directly from the conventional hydration of CAC. The reaction of CA, the main reactive clinker phase in CAC results in the eventual formation of stable cubic phase (C_3AH_6) through the formation of metastable hexagonal phases, CAH_{10} or C_2AH_8 as shown in the following equations [19,20].

$$CA + 10H \rightarrow CAH_{10} \quad (1)$$

$$2CA + 11H \rightarrow C_2AH_8 + AH_3 \quad (2)$$

$$2CAH_{10} \rightarrow C_2AH_8 + AH_3 + 9H \quad (3)$$

$$3C_2AH_8 \rightarrow 2C_3AH_6 + AH_3 + 9H \quad (4)$$

From Equations (1)-(4), the hydration of CA to form C_3AH_6 can be summarised as Equation (5).

$$3CA + 12H \rightarrow C_3AH_6 + 2AH_3 \quad (5)$$

These equations show that, in the conventional hydration of CA, the formation of AH_3 should occur always along with the formation of metastable CAH_{10}, C_2AH_8 or stable C_3AH_6 in comparable amount. However, XRD data (Figure 1), did not show the presence of these phases, suggesting that these hydration pathways did not occur.

A possible explanation for the formation of AH_3 in the 0.40p/c series without the other conventional CAC hydrates is the formation of AH_3 along the amorphous binding phase.

It has been reported that sodium calcium orthophosphate (SCOP) gel, $NaCaPO_4 \cdot nH_2O$, was formed in the similar systems as a precursor phase of hydroxyapatite [5,13]. In the presence of sodium polyphosphate, CA may be consumed according to the following reaction to form SCOP gel,

$$CaO \cdot Al_2O_3 + NaPO_3 + (3 + n)H_2O \rightarrow NaCaPO_4 \cdot nH_2O + 2Al(OH)_3 \qquad (6)$$

Equation (6) shows that the reaction of CA can result in AH_3 without forming other conventional CAC hydration products. The SCOP gel cannot be observed in the X-ray diffractograms, because it is amorphous [5].

3.2. Effect of water on product phases

Figures 3 and 4 show mass loss (wt%) and differential mass loss (wt%/°C) as a function of temperature for the 0.40p/c and the 1.14p/w series, in comparison with CAP_{ref}. With respect to CAP_{ref}, the main mass loss observed at 40 – 150°C with a broad peak in the differential curve could correspond to the loss of free water, as well as the loss of water loosely bonded with the amorphous SCOP gel [5,9,12,13]. The small mass loss in the region of 220 – 300°C corresponds to the dehydration of gibbsite, AH_3 [21]. This suggests that gibbsite presented in a small amount or in a poorly crystallized form in the CAP_{ref}, and was not positively detected in the XRD.

When the amount of mixing solution is increased with a constant amount of sodium polyphosphate in the 0.40p/c series, the mass loss of free water and water loosely bonded with the amorphous SCOP gel at 40 – 150°C increased first (CAP_{50w}), but then, decreased according to an increase of w/c ratio (CAP_{75w} and CAP_{100w}). On the other hand, the mass

loss attributed to AH_3 at 220 – 320°C increased and separated into two peaks with the increased amounts of mixing solution. The mass loss events at 220 – 240 and 240 – 320°C were clearly observable in CAP_{100w}. A similar behavior of a synthetic gibbsite at corresponding temperatures has been reported with DTA data [22], where the event at 220 – 240°C is attributed to the loss of non-hydrogen bonded hydroxyl groups and that at 240 – 320°C to the loss of water from gibbsite, part of which resulting in the formation of boehmite (γ-AlOOH). A small mass loss observed between 500 – 550°C is attributed to the dehydroxylation of the earlier formed boehmite. These results suggest that increased mixing solution with a constant amount of sodium polyphosphate promotes the formation of gibbsite and decrease in the free water and the water bonded with the amorphous SCOP gel, possibly because some of water was used to form gibbsite.

When the amount of mixing solution is increased at a constant concentration of sodium polyphosphate in the 1.14p/c series, the mass loss of free water and water bonded with the amorphous SCOP gel at 40 – 150°C increased with increasing amount of mixing solution. On the other hand, the mass loss of gibbsite at 220 – 320°C did not show any significant change. It appears that increasing amount of mixing solution only influences the amount of free water and water loosely bonded with the amorphous SCOP gel when the concentration of sodium polyphosphate in the mixing solution is constant. It did not contribute to the increased formation of gibbsite, even if amount of the mixing solution increased. The consumption of CA appears to depend on the concentration of sodium polyphosphate in the mixing solution. These results are in good agreement with the XRD results. The increase in gibbsite was observed in the 0.40p/c series, whereas the 1.14p/w series did not show the observable formation of gibbsite or any other crystalline hydrate phases.

Figure 5 illustrates the mass loss up to 150°C and that between 220 and 320°C as a function of the w/c ratio both for the 0.40p/c and the 1.14p/w series. With respect to the 0.40p/c series (open circle), the mass loss up to 150°C behaved like inverted parabolic curve (Figure 5 a), but the mass loss between 220 and 320°C showed a linear increase (Figure 5 b): the straight line is drawn by least square method ($R^2 = 0.97$). The exact cause of the inversed parabolic behavour for the free water and water loosely bonded with the amorphous gel phase is unclear, but must be related to the formation of gibbsite, as the mass loss between 220 and 320°C attributed to the gibbsite formation gradually increases. It appears that the formation of gibbsite takes some of the free water and water loosely bonded with the amorphous gel.

This observation can provide some insight into the behavior of alumina component in relation to the amorphous gel phase in CAP systems. Chavda *et al.* mentions the formation of C-A-P-H type gel, suggesting alumina component as a part of the amorphous gel phase [9], whereas Sugama and Carciello conclude a formation of alumina gel separated from the amorphous SCOP gel phase [5]. The data obtained in the present investigation suggests that both of these can happen, depending on the concentration of sodium polyphosphate in the mixing solution. A possible explanation is, when the concentration is high, *i.e.,* CAP_{ref} (same composition as Chavda *et al.* [9]), alumina component can stay as a part of the amorphous gel, but it can precipitate as gibbsite when the concentration of sodium phosphate in the solution becomes low, simultaneously resulting in some reduction of water by the consumption of free water and water loosely bonded with the amorphous SCOP gel.

With respect to the 1.14p/w series (closed circle), the mass loss up to 150°C showed a linear increase (Figure 5a): a straight line was drawn by a least square method ($R^2 = 0.99$).

On the other hand, the mass loss between 220 and 320°C did not show any observable change with the increase in the w/c ratio (Figure 5b). The linear increase in the mass loss up to 150°C shows an enhancement of the free water and water loosely bonded with the amorphous SCOP gel, likely suggesting a mild increase in the amorphous gel formation. Since the high concentration of sodium polyphosphate in the mixing solution was maintained in this series (1.14p/w series) and the consumption of CA was limited, the gibbsite formation was not increased, even if the amount of the mixing solution was increased.

3.3. Effect of water on bonding in the product phases

Figure 6 shows the ATR-FT/IR spectra for the raw materials (Secar® 51 and sodium polyphosphate) and the CAP samples (0.40p/c and 1.14p/w series). With respect to the raw materials (Figure 6a), the most obvious signals on Secar® 51 are the absorption bands in the region of 900 – 650 cm^{-1}. The bands from 900 - 750 cm^{-1} are attributed to the stretching vibration (υ) of Al-O in AlO_4 groups, while the bands at 750 - 600 cm^{-1} are associated with those in AlO_6 groups [23]. The peak at 1020 cm^{-1} corresponds to the bending vibration (δ) of OH groups in AH_3 [24]. Sodium polyphosphate shows the absorption bands for P=O (1260 cm^{-1}), P-O (1080 cm^{-1}), P-O-P stretching mode (980 and 864 cm^{-1}), and a region of double absorption band for δ P-O-P mode (780 – 710 cm^{-1}) [5,13,25].

With respect to the CAP_{ref} (Figures 6b and 6c), the peak at 1260 cm^{-1} corresponding to P=O double bonds disappeared, and a new band at 1024 cm^{-1} was observed, corresponding to orthophosphate ($R\text{-}PO_4$) [5]. Orthophosphates can show strong and broad peaks ranging from 1150 to 1000 cm^{-1} [25-27]. These bands would also coincide

with the formation of SCOP gel, as reported by Sugama and Carciello [5]. The result indicates that the sodium polyphosphate used in the CAP_{ref} was consumed by acid-base reaction with Secar® 51 and orthophosphate gel was formed.

In the 0.40p/c series (Figure 6b), the band at 1024 cm^{-1} corresponding to R-PO_4 becomes more intense as the amount of the mixing solution is increased with a constant amount of sodium polyphosphate. This peak could also be overlapping with the bending vibration (δ) of OH groups in AH_3 to be observed at 1020 cm^{-1} [20]. On the other hand, the bands at 910 and 1080 cm^{-1} corresponding to $H_2PO_4^-$ becomes less intense with the increase in water. These results indicate that increasing mixing solution with constant amount of sodium polyphosphate led to an increase in R-PO_4 and AH_3, but to a decrease in $H_2PO_4^-$.

In the 1.14p/w series (Figure 6c), the band at 1260 cm^{-1} corresponding to P=O became observable when the mixing solution is increased at a constant concentration of sodium polyphosphate. The balance of the absorption bands at 1080, 1024, and 910 cm^{-1} did not show any observable change among the CAP_{ref}, CAP_{57p}, CAP_{86p}, and CAP_{114p} although the intensity of the peaks appears to gradually increase. The observation of P=O bonding shows that a significant amount of sodium polyphosphate remained in the system without fully consumed when it is increased together with water at a constant concentration, suggesting a limited reaction of CAC clinkers necessary for the consumption of sodium poly phosphate. This is consistent with the XRD data previously discussed.

3.4. Effect of water on microstructure

Figure 7 shows backscattered electron (BSE) and elemental mapping (Na, P, Al, Ca) images for the CAP_{ref}, CAP_{100w} and CAP_{114p}. In the BSE images, microcracks are shown

in black lines and unreacted CAC clinker phases in light grey. The microcracks is considered to be formed by the shrinkage of the amorphous binding phase, because of the initial exothermal acid-base reaction between Secar® 51 and sodium polyphosphate and successive cooling down of the system [8,12].

The BSE image for CAP_{100w} clearly shows less microcracks and unreacted CAC clinker phases compared with those for CAP_{ref} and CAP_{114p}. The increased reaction of CAC or CA (the main clinker phase of Secar® 51) is consistent with the XRD results shown in Figure 1. It appears that the increase in the mixing solution (without changing the amount of sodium polyphosphate) can improve the microstructure of the system by promoting the reaction of CA. In this particular series (0.40p/c series), the increased formation of gibbsite and the reduction of water bonded with the amorphous gel phase were identified (Figures 3 and 5), and they must have also contributed to the improvement of the microstructure. This is interesting, as the reduction of microcracks in the CAP systems has been reported so far only by curing the system at elevated temperatures [13].

According to the elemental mapping, Na and P clearly exist in the amorphous matrix phase in all of CAP_{ref}, CAP_{100w} and CAP_{114p}, while Al and Ca exist both in the amorphous matrix and unreacted CAC phases. It is, however, noticeable that more Al and Ca are dispersed in the matrix phase in the CAP_{100w} (0.40p/c series), confirming the enhanced reaction of CA and corresponding inclusion of Al and Ca in the matrix phase.

4. Conclusions

The present study investigated the effects of the amount of mixing solution on the characteristics of the CAP system. When the mixing solution was increased with a

constant amount of sodium polyphosphate, the consumption of monocalcium aluminate in the CAC was enhanced, resulting in the increased formation of gibbsite and the reduced free water and water bonded with the amorphous gel phase. No crystalline hydration products with calcium was identified, suggesting that it is forming a part of the amorphous gel phase. On the other hand, when the mixing solution was increased with constant concentration of sodium polyphosphate, the enhanced consumption of monocalcium aluminate was not observed. Neither gibbsite nor any other crystalline hydration products was identified in the products in this series. In addition, unreacted sodium polyphosphate remained in the CAP.

The data obtained in the present investigation suggests that aluminium ions can take a part of the amorphous gel phase or precipitate as gibbsite when the amount of mixing solution is increased, depending on the concentration of sodium polyphosphate in the mixing solution. When the concentration is high, aluminium ions can stay as a part of the amorphous gel, but it can precipitate as gibbsite when the concentration of sodium phosphate in the solution becomes low, resulting in a reduction of water from the amorphous gel phase. Both the increased formation of gibbsite and the reduction of water from the amorphous gel phase appears to contribute towards reducing the microcracks of the system. This would be beneficial for research and application of CAP-like chemically-bonded phosphate cements and ceramics in the fields of environment, nuclear, civil engineering and so on.

Acknowledgements

This work was funded by the Engineering and Physical Sciences Research Council, UK (EP/N017684/1) and the Japan Science and Technology Agency, Japan (research grant No. 273604).

References

[1] A.D. Willson and J.W. Nicholson, Acid-Base Cements, Cambridge University Press, 1993.

[2] A.S. Wagh, S.Y. Sayenko, A.N. Dovnya, V.A. Shkuropatenko, R.V. Tarasov, A.V. Rybka, A.A. Zakharchenko, Durability and Shielding Performance of Borated Ceramicrete Coatings in Beta and Gamma Radiation Fields, *J. Nucl. Mater.*, **462** (2015) 165-172.

[3] A.S. Wagh, Recent Progress in Chemically Bonded Phosphate Ceramics, ISRN ceramics, **Vol. 2013**, Article ID 983731 (2013) 20 pages.

[4] T. Sugama and N.R. Carciello, Strength Development in Phosphate-Bonded Calcium Aluminate Cements, *J. Am. Ceram. Soc.*, **74**, 5 (1991) 1023-1030.

[5] T. Sugama and N.R. Carciello, Sodium Phosphate-Derived Calcium Phosphate Cements, *Cem. Concr. Res.*, **25**, 1 (1995) 91-101.

[6] W. Ma, P.W. Brown, Mechanical behaviour and microstructural development in phosphate modified high alumina cement, *Cem. Conc. Res.*, **22** (1992) 1192-1200.

[7] W. Ma, P.W. Brown, Hydration of sodium phosphate-modified high alumina cement, *J. Mater. Res.*, 9, 5 (1994) 1291-1297.

[8] M.A. Chavda, H. Kinoshita, J.L. Provis, Phosphate modification of calcium aluminate cement to enhance stability for immobilisation of metallic wastes, *Adv. Appl. Ceram.*, **113**, 8 (2014) 453-459.

[9] M.A. Chavda, S.A. Bernal, D.C. Apperley, H. Kinoshita, J.L. Provis, Identification of the hydrate gel phases present in phosphate-modified calcium aluminate binders, *Cem. Conc. Res.*, **70** (2015) 21-28.

[10] H. Kinoshita, P. Swift, C. Utton, B. Carro-Mateo, G. Marchand, N. Collier, N. Milestone, Corrosion of aluminium metal in OPC- and CAC-based cement matrices, *Cem. Concr. Res.*, **50** (2013) 1-8.

[11] J.M. Fernandez, I. Navarro-Blasco, A. Duran, R. Sirera, J.I. Alvarez, Treatment of toxic metal aqueous solutions: encapsulation in a phosphate-calcium aluminate matrix, *J. Environ. Manag.*, **140** (2014) 1-13.

[12] P. Swift, H. Kinoshita, N.C. Collier, C.A. Utton, Phosphate modified calcium aluminate cement for radioactive waste encapsulation, *Adv. Appl. Ceram.*, **112** (2013) 1-8.

[13] I. Garcia-Lodeiro, K. Irisawa, F. Jin, Y. Meguro, H. Kinoshita, Reduction of water content in calcium aluminate cement with/out phosphate modification for alternative cementation technique, *Cem. Conc. Res.*, **109** (2018) 243-253.

[14] K.K. Sideris, M. Konsta-Gdoutos, Influence of the Water to Cement Ratio W/C on the Compressive Strength of Concrete – An Application of the Cement Hydration Equation to Concrete, *Appl. Compos. Mater.*, **3** (1996) 335-343.

[15] J. Skalny, J.C. Phillips, D.S. Cahn, Low Water to Cement Ratio Concretes, *Cem. Concr. Res.*, **3** (1973) 29-40.

[16] L.K.A. Sear, J. Dews, B. Kite, F.C. Harris, J.F. Troy, Abrams law, air and high water-to-cement ratios, *Const. Build. Mater.*, **10**, 3 (1996) 221-226.

[17] A. Zhang, L. Zhang, Influence of Cement Type and Water-to-Cement Ratio on the Formation of Thaumasite, *Adv. Mater. Sci. Eng.*, 7643960 (2017) 6 pages.

[18] I. Navarro-Blasco, A. Duran, M. Perez-Nicolas, J.M. Fernandez, R. Sirera, J.I. Alvarez, A safer disposal phosphate coating sludge by formation of an amorphous calcium phosphate matrix, *J. Environ. Manage.*, **159** (2015) 288-300.

[19] R.N. Edmonds, A.J. Majumdar, The Hydration of Monocalcium Aluminate at Different Temperatures, *Cem. Conc. Res.*, **18** (1988) 311-320.

[20] V.S. Ramachandran, R.F. Feldman, Hydration Characteristics of Monocalcium Aluminate at a Low Water/solid ratio, *Cem. Conc. Res.*, **3** (1973) 729-750.

[21] V. Balek, J. Subrt, J. Rouquerol, P. Llewellyn, V. Zelenak, I.M. Bountsewa, et al., Emanation thermal analysis study of synthetic gibbsite, *J. Therm. Anal. Calorim.*, **71** (2003) 773-782.

[22] J.T. Kloprogge, H.D. Ruan, R.L. Frost, Thermal decomposition of bauxite minerals: infrared emission spectroscopy of gibbsite, boehmite and diaspore, *J. Mater. Sci..*, **37** (2002) 1121-1129.

[23] P. Tarte, Infra-red spectra of inorganic aluminates and characteristic vibrational frequencies of AlO_4 tetrahedra and AlO_6 octahedra, *Spectrochim. Acta*, **23A** (1967) 2127-2143.

[24] A. Hidalgo, J.L. Garcia, M. Cruz Alonso, L. Fernandez, C. Andrade, Microstructure development in mixes of calcium aluminate cement with silica fume or fly ash, *J. Therm. Anal. Cal.*, **96** (2009) 335-345.

[25] T. Sugama, M. Allan, J.M. Allan, Calcium phosphate cements prepared by acid-base reaction, *J. Am. Ceram. Soc.*, **75**, 8 (1992) 2076-2087.

[26] Y.M. Moustafa, K. El-Egili, Infrared spectra of sodium phosphate glasses, *J. Non-Cryst. Solids*, **240** (1998) 144-153.

[27] F.A. Miller, C.H. Wilkins, Infrared spectra and characteristic frequencies of inorganic ions, *Anal. Chem.*, **24**, 8 (1952) 1253-1294.

Table 1. Oxide composition of Secar® 51 [13].

Oxides	Al_2O_3	CaO	SiO_2	TiO_2	Fe_2O_3	MgO	SO_3	K_2O+Na_2O
(wt%)	50.77	38.39	4.83	2.04	1.82	0.40	0.24	0.63

Table 2. The compositions of the CAP samples in this study.

Sample	Mass (g)			Mass ratio (g/g)		
	Cement	Mixing solution				
	c	p	w	p/c	p/w	w/c
CAP_{ref}	100	40	35	0.40	1.14	0.35
0.40p/c series						
CAP_{50w}	100	40	50	0.40	0.80	0.50
CAP_{75w}	100	40	75	0.40	0.53	0.75
CAP_{100w}	100	40	100	0.40	0.40	1.00
1.14p/w series						
CAP_{57p}	100	57	50	0.57	1.14	0.50
CAP_{86p}	100	86	75	0.86	1.14	0.75
CAP_{114p}	100	114	100	1.14	1.14	1.00

c: cement; p: sodium polyphosphate; w: distilled water; p/c: sodium polyphosphate to cement weight ratio; p/w: sodium polyphosphate to distilled water weight ratio; w/c: distilled water to cement weight ratio.

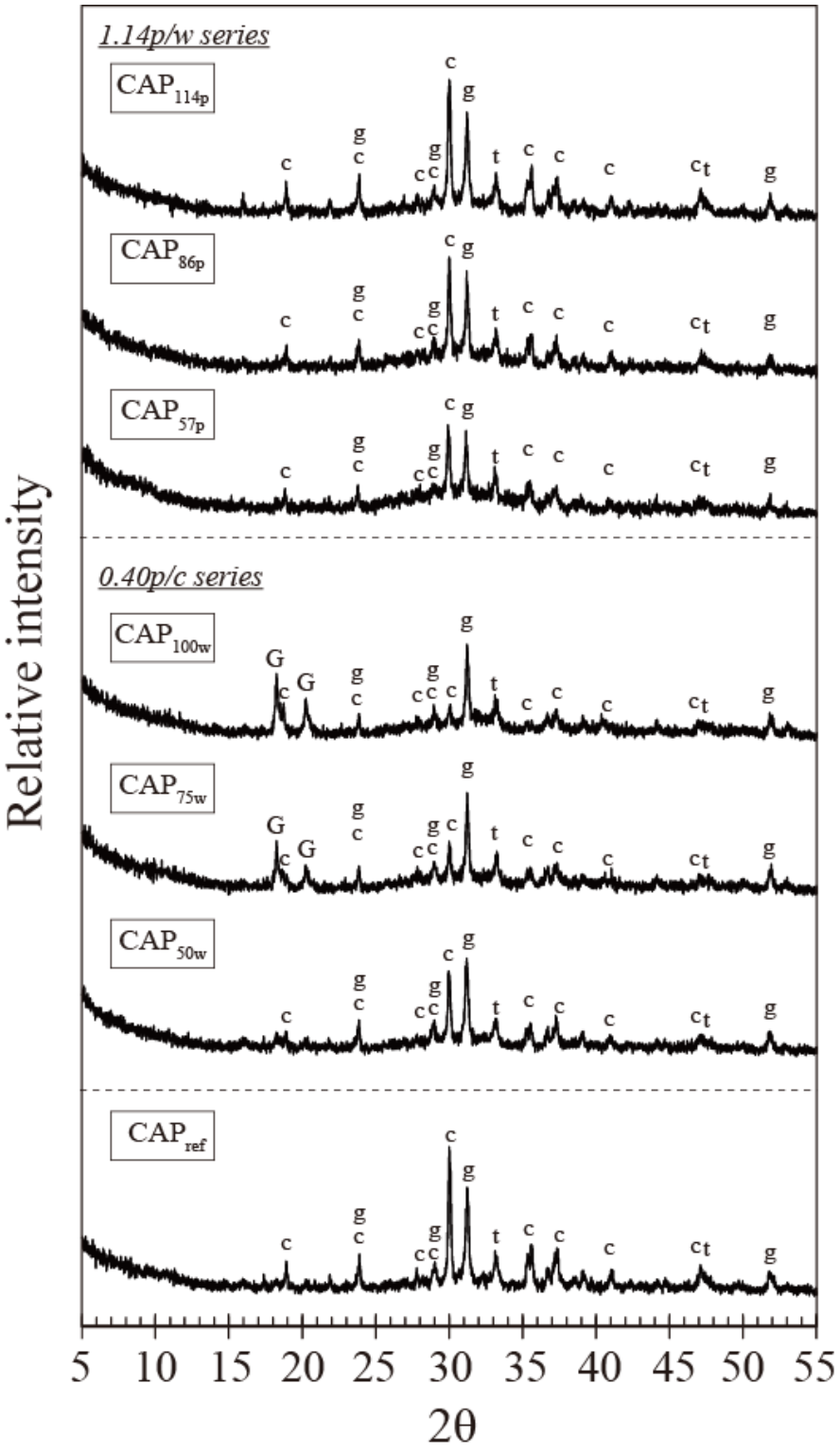

Figure 1. X-ray diffractograms for the CAP samples.

(c: CA, g: C_2AS, t: CT, G: AH_3)

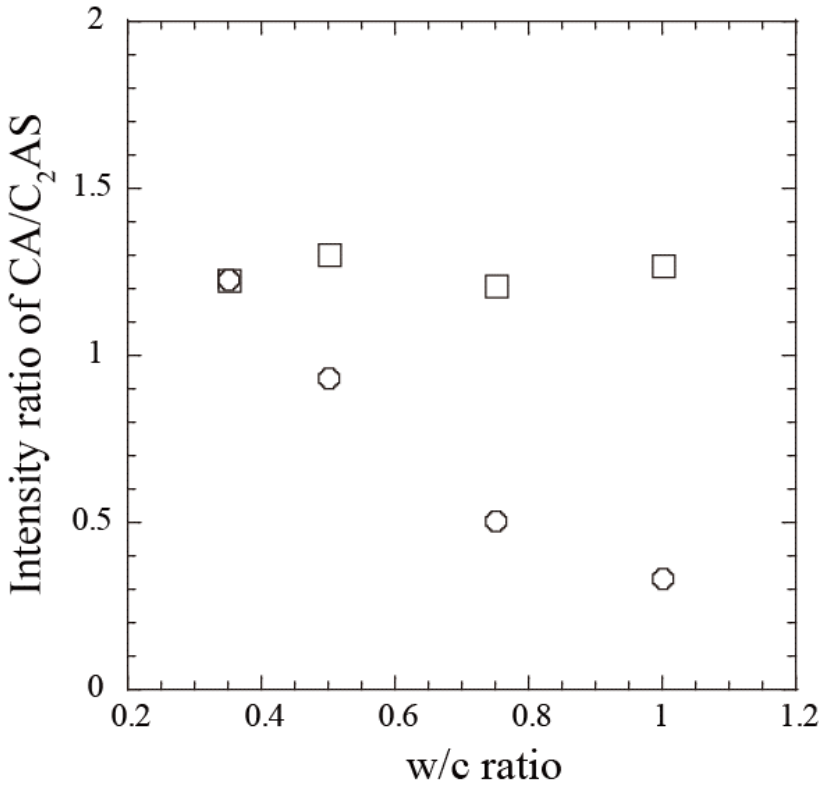

Figure 2. Intensity ratio of CA (29.9°) to C_2AS (31.2°) as a function of w/c ratio.

(circle, 0.40p/c series; square, 1.14p/w series)

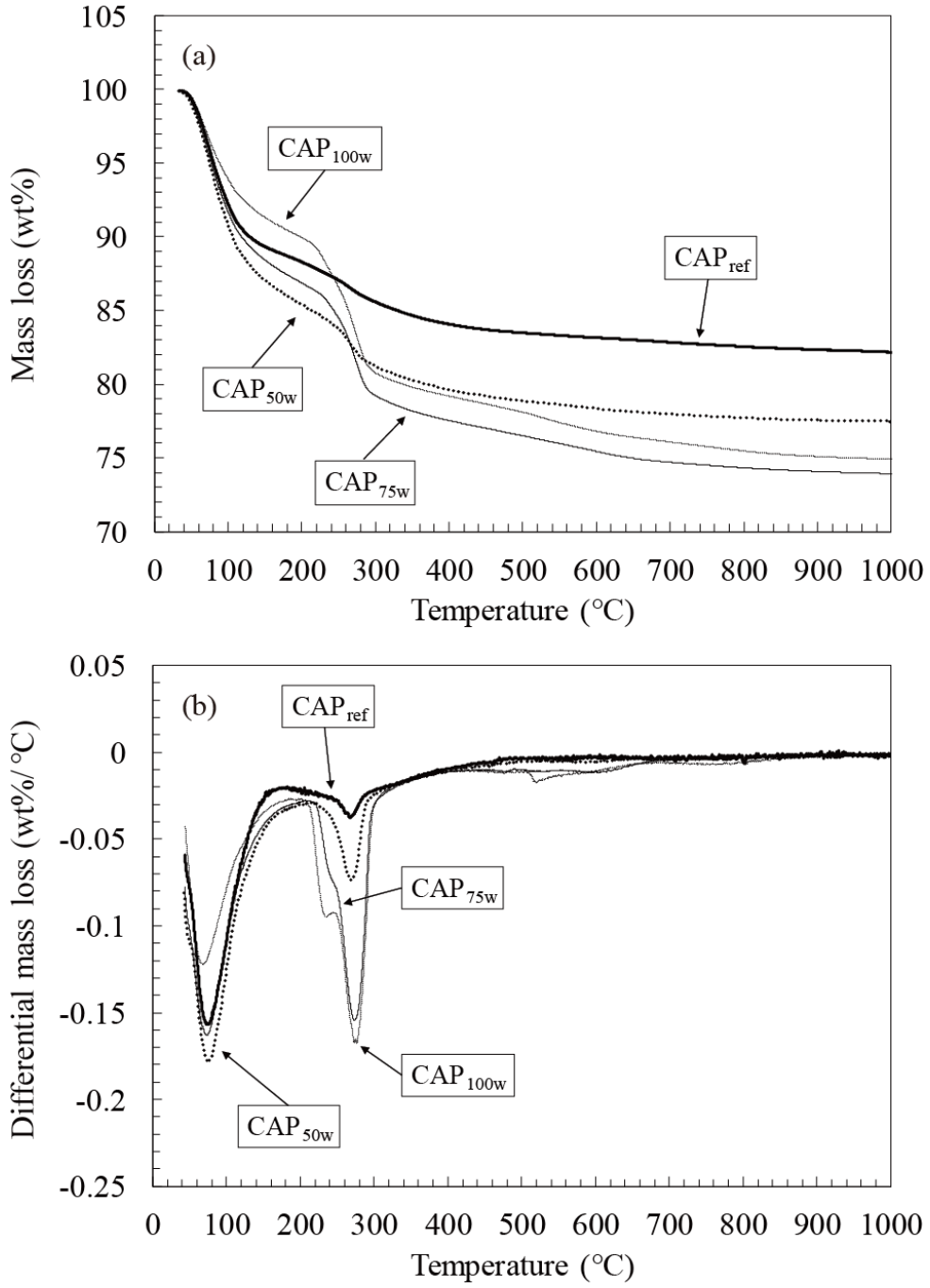

Figure 3. (a) Mass loss (wt%) and (b) differential mass loss (wt%/°C) as a function of temperature for CAP_{50w}, CAP_{75w}, and CAP_{100w} in 0.40p/c series, compared with CAP_{ref}. (Bold solid line: CAP_{ref}; Bold dotted line: CAP_{50w}; solid line: CAP_{75w}; dotted line: CAP_{100w})

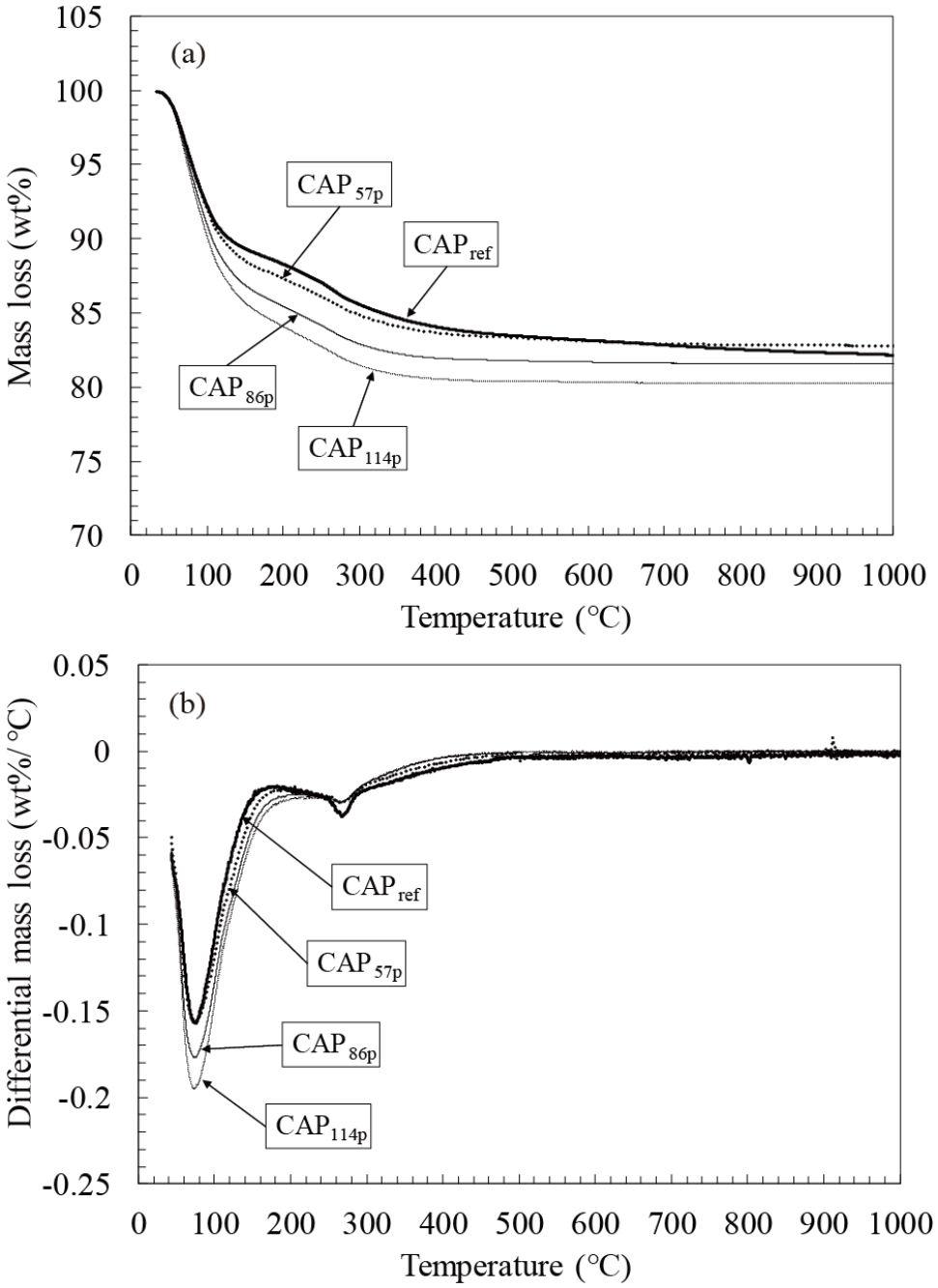

Figure 4. (a) Mass loss (wt%) and (b) differential mass loss (wt%/°C) as a function of temperature for CAP_{57p}, CAP_{86p}, and CAP_{114p} in 1.14p/w series, compared with CAP_{ref}. (Bold solid line: CAP_{ref}; Bold dotted line: CAP_{57p}; solid line: CAP_{86p}; dotted line: CAP_{114p})

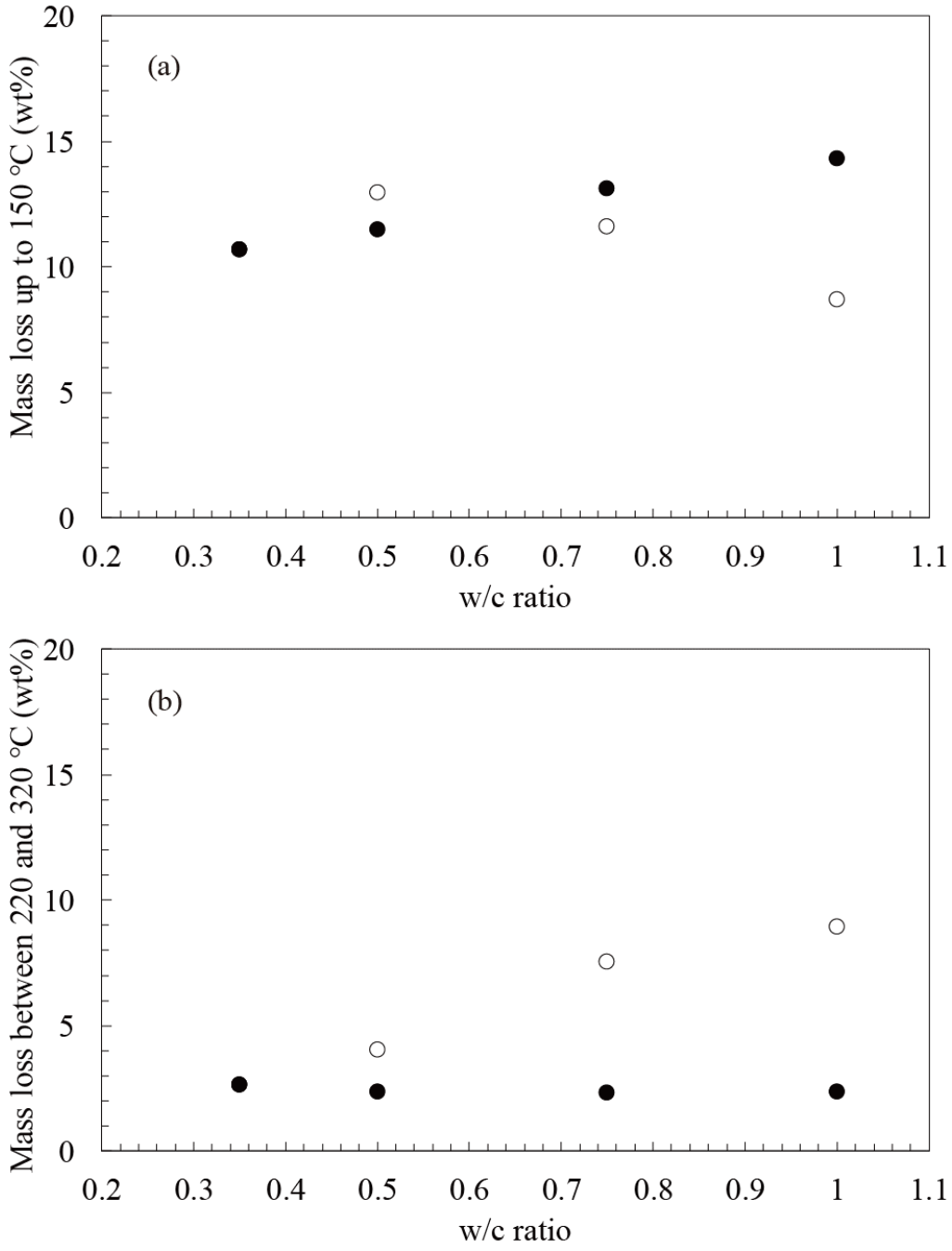

Figure 5. The mass loss (a) up to 150°C and (b) between 220 and 320°C as a function of the w/c ratio for the 0.40p/c (open circle) and 1.14p/w series (closed circle).

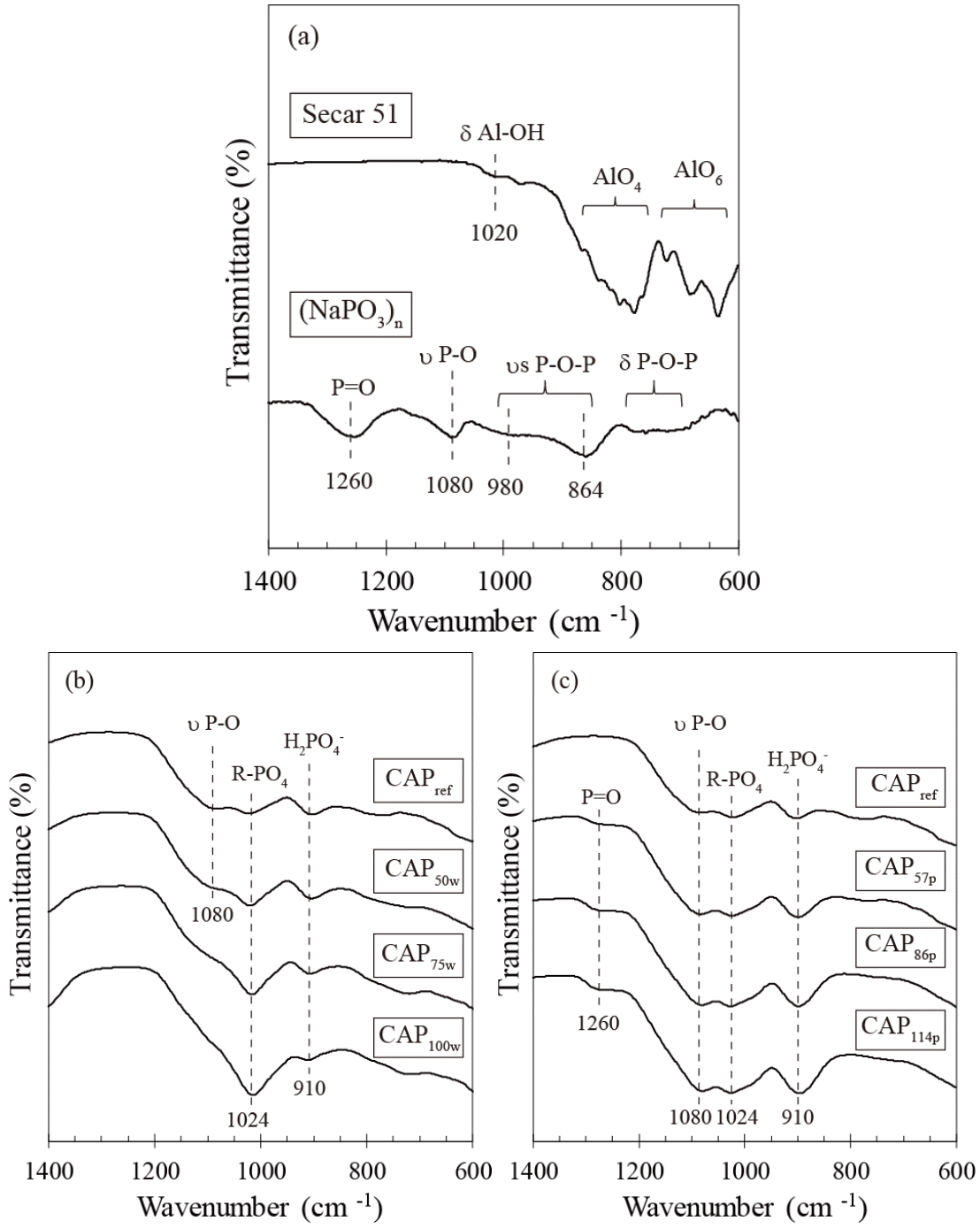

Figure 6. ATR-FT/IR spectra for (a) raw materials, (b) the CAP samples in the 0.40p/c series, and (c) the CAP samples in the 1.14p/w series.

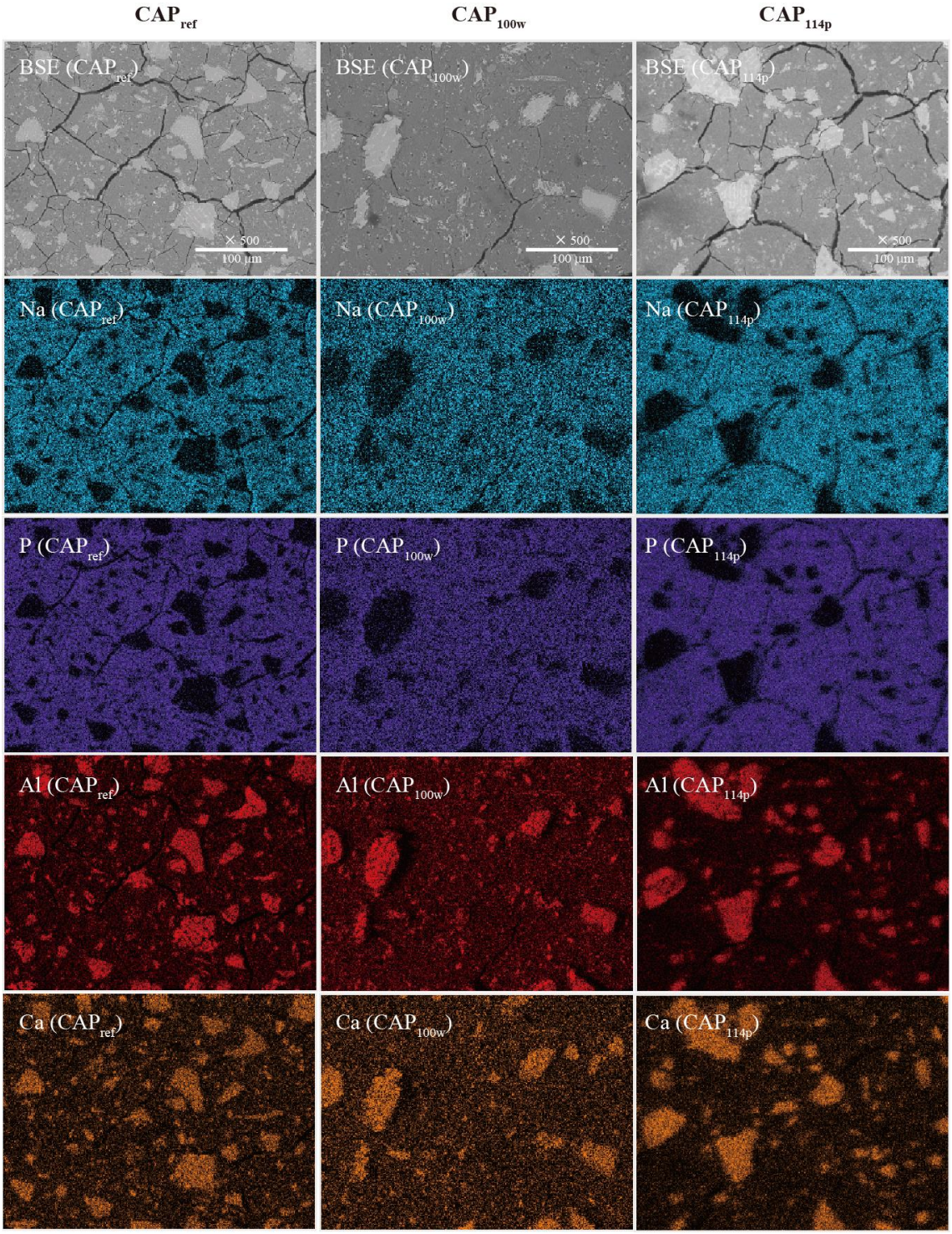

Figure 7. Backscattered electron (BSE) and elemental mapping (Na, P, Al, Ca) images for the CAP_{ref}, CAP_{100w}, and CAP_{114p}.